Journal of Pharmaceutical and Biomedical Analysis Open 2 (2023) 100019

Contents lists available at ScienceDirect

Journal of Pharmaceutical and Biomedical Analysis Open

journal homepage: www.journals.elsevier.com/journal-of-pharmaceutical-and-biomedical-analysis-open

Advances in surface plasmon resonance biosensors for medical diagnostics: An overview of recent developments and techniques

G.I. Janith [a], H.S. Herath [a], N. Hendeniya [a], D. Attygalle [a,*], D.A.S. Amarasinghe [a], V. Logeeshan [b], P.M.T.B. Wickramasinghe [c], Y.S. Wijayasinghe [c]

[a] Department of Materials Science and Engineering, University of Moratuwa, Sri Lanka
[b] Department of Electrical Engineering, University of Moratuwa, Sri Lanka
[c] Department of Biochemistry and Clinical Chemistry, University of Kelaniya, Sri Lanka

ARTICLE INFO

Keywords:
Surface plasmon resonance
Plasmon-based sensors
Medical diagnostics
Biosensors

ABSTRACT

Over the last two decades, surface plasmon resonance (SPR) sensors have advanced significantly, becoming an important tool in disciplines such as biosensing, chemical sensing, and material characterization. SPR has gained popularity in biosensing because of its great sensitivity and specificity in detecting biomolecular interactions. This review provides an overview of the recent developments of the SPR biosensor technology and its applications in medical diagnostics. To provide an up-to-date overview of the area, the review includes the most recent works from the last decade. Furthermore, it explores various configurations (prism, grating, fiber optic, waveguide modulated) and wave properties (angle, wavelength, phase) being tracked for sensing together with strategies for enhancing sensitivity and selectivity through mechanisms such as surface coatings, sensing mediums, and immobilization techniques.

1. Introduction

Early and accurate diagnosis of a disease and its causative pathogens is an important step toward appropriate intervention measures. Early detection of diseases, particularly chronic diseases, while they are asymptomatic, they necessitate specialized diagnostic testing. Early detection enables a wider range of cures and longer survival. Failure to do so can result in long-term complications, for example cervical cancer from high-risk strains of the human papillomavirus, and chronic hepatitis and liver cancer from both hepatitis B and hepatitis C [1].

Early detection via traditional diagnostic techniques requires excessive examination schedules and medical resources and it is also inevitably costly. Biosensors play a major role in making early detection a reality. Nowadays a biosensor is a ubiquitous tool in biomedical diagnosis and is also an integral part of various areas such as point-of-care (POC) monitoring and treatment, environmental monitoring, food control, drug discovery, and biomedical research [2]. A variety of techniques can be utilized to develop biosensors. The coupling of high-affinity biomolecules with these sensors allows sensitive and selective detection for a variety of analytes. A generic biosensor contains three main elements target, recognition, and transducing element. The target is the analyte molecule to be detected and it is captured by a recognition element via special interactions. The recognition element then undergoes a chemical or physical change. This change is then converted to a readable signal with the help of a transducer.

Conventional transducing techniques that utilize electrochemical, chromatographical, or mass-sensitive properties have undergone extensive development. As a result, a variety of commercially available sensors have been developed in recent years [3–6]. Plasmonic-based sensors have been under development for over 40 years and a variety of devices have been commercially available. Compared to conventional sensors they have a few advantages such as real-time monitoring capabilities, label-free detection, high sensitivity, short response time, and high reusability. Surface-enhanced fluorescence (SEF) spectroscopy or plasmon-enhanced fluorescence is a technique where a plasmonic nanomaterial has been used to increase the fluorescence intensity of a fluorophore material [7]. Usually, this is achieved by placing the fluorophore in proximity to a metallic nanoparticle. As a result, the fluorophore experiences an increased electric field hence, an enhanced emission. SEF is widely used to sense a variety of analytes in POC devices [8,9].

Surface-enhanced Raman spectroscopy (SERS) has been a dominant

* Corresponding author.
E-mail address: dattyga@uom.lk (D. Attygalle).

https://doi.org/10.1016/j.jpbao.2023.100019
Received 3 July 2023; Received in revised form 3 September 2023; Accepted 8 September 2023
Available online 9 September 2023

analytical method in the last few decades due to its high selectivity by unique fingerprint signatures, easy sample preparation, lesser interference from analyte medium, and capability of single molecule detection [10]. A plasmonic nanostructure possesses an enhanced localized Electromagnetic field due to the Localized Surface plasmonic resonance (LSPR) effect, this field affects the Raman signal by enhancing the Raman scattering cross-section if the material is near. This enhancement is due to a combination of two effects EM enhancement and chemical enhancement. First, as a contribution of order 10^4–10^8 while the second effect is around 10–100 [10].

Surface plasmons, also often known in the literature as surface plasmon polaritons (SPPs) or surface plasma waves (SPWs), are electromagnetic excitations in the form of charge density oscillations of the free electron gas. Surface Plasmon Resonance (SPR) is an optical phenomenon that provides a non-invasive, label-free means of observing binding interactions between analyte and biomolecule. With the introduction of SPR for gas detection and biosensing by Nylander and Liedberg [11], SPR-based biosensors are a field with growing interest.

SPR is an optical sensing technique where the target molecule is detected through the refractive index (RI) change that occurs near the sensing layer as a result of the presence of a new substance i.e., analyte molecules. This change in RI is identified through the changes in the electromagnetic resonance of the evanescence wave. The characteristics of the SPP wave are highly sensitive to the dielectric layers and their changes in the sensor. SPR sensors need a coupling mechanism to function. Initially, this was achieved through prism coupling with the introduction of the Kretschmann configuration [12]. Over time this has evolved and studies with other coupling mechanisms such as optical fiber, waveguide, and grating-based sensors can be seen.

SPR has several advantages as a biosensing technique. SPR allows measuring the binding kinetics and affinity of biomolecules in real-time. SPR is known as a label-free method, and it makes the technique more appealing for virus detection as it eliminates the common problem of weakening binding due to the label and facilitates direct measurement of binding kinetics. Other than enhanced sensitivity with reported detection levels of pg/μL, SPR also provides a quantitative response, the ability to miniaturize, and integrated usage with other techniques like surface plasmon resonance imaging (SPRi) [13].

LSPR is a recent extension of plasmonic sensing which enables higher sensitivity levels. In LSPR, nanostructures with a much smaller size compared to incident light wavelength are used for sensing. Light interacts with the nanoparticles (NP) of different shapes such as nanorods, nanospheres, and nanoshells enabling plasmons to oscillate locally around the NP. The LSPR is sensitive to RI changes in the surrounding medium other than to the parameters such as the shape and size of NPs. Thus, a change in the medium can be tracked through the wave property variation such as LSPR wavelength shift or angle shift. LSPR provides additional advantages such as a higher aspect ratio increasing sensitivity and improved flexibility as LSPR wavelength can be tuned by controlling the NP characteristics. Furthermore, recent advancements include LSPR-based colorimetric sensing techniques and integration with techniques like fluorescence, Raman, and IR spectroscopy [8,14,15].

However, there are limitations to the SPR as a biosensing technique with sensitivity, detection of small biomolecules, and cost of production. Thus, the current trends of SPR developments mainly focus on enhancing the sensitivity beyond current limits allowing the detection of small biomolecules and increasing functionality through multiplexing so the technology can be used for the detection of multiple analytes at the same time. This review seeks to provide a thorough overview of the present state of SPR biosensor technology and its applications in medical diagnostics using the studies from the last ten years (from 2013 to 2022). Furthermore, the review will go through the various configurations available for SPR biosensing, such as prism, grating, fiber optic and waveguide modulated and various wave properties that are being tracked for sensing such as angle, wavelength and phase. This review also discusses strategies for increasing sensitivity and selectivity, such as using different surface coatings and sensing mediums and immobilization techniques. Moreover, we have included a detailed table (Table 1) that summarizes various SPR sensors and their applications in medical diagnostics to better understand the versatility of SPR technology in the area. The table provides information on the various SPR sensor setups, sensing layer and specific property that has been tracked to detect changes together with the diseases they have been used to detect, the receptor types used, and the level of detection attained.

2. Theoretical background

Surface plasmon resonance is a phenomenon arising from light and free electron interaction in a metal – dielectric interface (Fig. 1). Under certain conditions the surface electron oscillation resonates with the incident electromagnetic field and as a result photon loses a significant amount of its energy. This energy transfer takes place in a specific resonance wavelength of light and the momentum of surface plasmon and the photon also must match. The surface plasmons are heavily localized to the dielectric interface and they propagate parallel to the interface. In perpendicular direction to the interface the amplitude of SPP evanescent wave decay exponentially. The coupling between the incident light and plasmons is highly sensitive to the RI immediate to the metal surface. A change in this RI in return shifts the resonant angle of the light or resonant wavelength or other characteristics of the incident light. Such changes can be calibrated to the change of RI [16].

Principles and fundamental theories behind SPPs and SPR can be explained as follows. The physical properties of SPPs are governed by maxwell's equations. Fundamental equations can be simplified down to the following form.

$$\nabla^2 E - \frac{\varepsilon}{c^2}\frac{\partial^2 E}{\partial t^2} = 0 \tag{1}$$

This is the central equation of electromagnetic wave theory. This equation needs be solved separately in regions of uniform dielectric constant ε with appropriate boundary conditions. To better cast the Eq. (1) into a form suitable for confined propagating waves, we can assume a time harmonic field for both electric and magnetic fields.

$$E(r,t) = E(r)e^{-i\omega t} \tag{2}$$

By inserting this into Eq. (1) yield the Helmholtz equation where $k_0 = \frac{\omega}{c}$.

$$\nabla^2 E + k_0^2 \varepsilon E = 0 \tag{3}$$

After settling down to a one-dimensional problem as $E(x,y,z) = E(z)e^{i\beta x}$ where β is called the propagation constant, the resultant expression is as follows:

$$\frac{\partial^2 E(z)}{\partial z^2} + \left(k_0^2 \varepsilon - \beta^2\right)E = 0 \tag{4}$$

A comparable equation exists for the magnetic field H as well. Solving this problem results in two sets of self-consistent solutions namely the transverse magnetic mode (TM or p mode) and the transverse electric mode (TE or s mode). Since SPPs only exist for TM polarization, the solutions are as follows. Fig. 1 represents the geometry of the problem.

For $z > 0$

$$H_y(z) = A_2 e^{i\beta x} e^{-k_2 z} \tag{5}$$

$$E_x(z) = iA_2 \frac{1}{\omega \varepsilon_0 \varepsilon_2} k_2 e^{i\beta x} e^{-k_2 z} \tag{6}$$

$$E_z(z) = -A_2 \frac{\beta}{\omega \varepsilon_0 \varepsilon_2} k_2 e^{i\beta x} e^{-k_2 z} \tag{7}$$

For $z < 0$

Table 1
SPR sensors for biosensing applications.

Ref.	Configuration	Receptor	Analyte	Level of detection/ sensitivity	materials	Wave property tracked
[69]	Plastic optical Fiber	Guinea pig tTG protein (Transglutaminase)	anti-transglutaminase antibodies)	LoD 30–3000 nM.	A thin gold layer	wavelength
[81]	Prism (Kretschmann configuration)	prolamin working group (PWG) gliadin	gluten peptides in urine	LoD of 1.72 ng/mL)	glass surface coated with 1 nm of Ti and 45 nm of Au	wavelength
[82]	Fiber optic	Probe DNA Sequence – 5′-CTT CTG TCT TGA TGT TTG TCA AAC-3′	Target DNA Sequence – 5′-GTT TGA CAA ACA TCA AGA CAG AAG-3′	1227 nm/RIU	Cu foil Graphene layer Au film	Wavelength
[70]	Fiber optic	staphylococcal protein A (SPA) modified with Rabbit antihuman IgG antibody	human immunoglobulin G (IgG)	Sensitivity – 0.096 dB/(μg/mL) LoD – 0.5 μg/mL	Graphene oxide on gold	Wavelength
[83]	optical fiber	biotinylated anti-CLU IgG and biotinylated anti-apoE IgG	Cancer biomarkers Apolipoprotein E Clusterin	Sensitivity - 740 nm/RIU, LoD – 4×10^{-5} RIU.	Silver	wavelength
[64]	Optical fiber	Carboxylic (COOH)	Ethanol solution	3061 nm/RIU	MoS2 nanosheets	wavelength
[67]	Optical fiber	Aptamer with NH_2	t- DNA, mis-DNA	DL 10 pM, 4461 nm/ RIU	3D Au/ Al_2O_3 multilayer composite hyperbolic metamaterial (HMM), a graphene film.	wavelength
[68]	Optical fiber	Polyclonal rabbit anti-Ara h1 antibodies	peanut allergen Ara h 1	0.09 ug/mL	Magnetite nanoparticles Gold	wavelength
[69]	Optical fiber	Guinea pig liver transglutaminase (tTG).	Anti-transglutaminase (anti-tTG)	30 nM and 3000 nM	Gold	wavelength
[42]	Prism coupling	-	biosensor for detection of urea and creatinine	1.4°/M in non-enzymatic urea samples. 4°/M in non-enzymatic creatinine samples. 16.2°/M in enzymatic urea samples. 10°/M in enzymatic creatinine samples.	gold	angle
[84]	Prism (Modified Kretschmann configuration)	immobilized ligands and	disease in the human teeth	104.744°/RIU	Ag, MXene, and the MoS2 layer.	angle
[56]	Grating coupled	peptide nucleic acid (PNA) probes	Mycobacterium tuberculosis (MT) DNA	LoD 0.26 pM	A sinusoidal grating with a bi-metallic layer (chromium (5 nm)/gold (40 nm))	angle
[57]	Grating	antibodies	tumor cells (CTCs	-	Titanium (5 nm) Gold (20 nm)	Angle
[75]	Waveguide	IgG	a-IgG	LoD 10 pM	Gold film Thiol linker PNIPAAm hydrogel film	Angle
[44]	prism	anti-17β-estradiol antibody	17β-estradiol	LoD – 0.0036 pM	Gold	Angle
[80]	Wave guide	Anti-CRP	C-reactive protein	0.3034 g/mL	Au-Ag Bi-metallic waveguide	Angle
[79]	Wave guide	Anti-Aβ42	Amyloid-β42	500 pg/mL	Ag layer Zns-SiO_2 waveguide Au layer	Angle
[85]	prism coupler sensor	rabbit anti-human immunoglobulin G (IgG). (Oxygen-containing functional groups)	Human and Mouse IgG	5–10 ng/mL	Graphene layer Cr-Au thin film Ta_2O_5 thin film	Phase
[43]	Prism	Concanavalin A	Xanthan gum	LoD 0.045 g/L	Gold	Intensity

Fig. 1. Geometry of a single interface of metal and a dielectric.

$$H_y(z) = A_1 e^{i\beta x} e^{-k_1 z} \tag{8}$$

$$E_x(z) = -iA_1 \frac{1}{\omega \varepsilon_0 \varepsilon_1} k_2 e^{i\beta x} e^{-k_1 z} \tag{9}$$

$$E_z(z) = -A_1 \frac{\beta}{\omega \varepsilon_0 \varepsilon_1} k_2 e^{i\beta x} e^{-k_1 z} \tag{10}$$

In both mediums the electric and magnetic fields are subjected to evanescent decay. Using the boundary conditions of H_y continuity and E_x continuity it can be shown that $A_1 = A_2$ and $\frac{k_2}{k_1} = -\frac{\varepsilon_2}{\varepsilon_1}$.

Further they must satisfy the equations.

$$k_1^2 = \beta^2 - k_0^2 \varepsilon_1 \tag{11}$$

$$k_2^2 = \beta^2 - k_0^2\varepsilon_2 \tag{12}$$

Combining these conditions, we arrive at the dispersion relation of SPPs.

$$\beta = k_0\sqrt{\frac{\varepsilon_1\varepsilon_2}{\varepsilon_1+\varepsilon_2}} \tag{13}$$

Fig. 2 illustrates the dispersion relation for a metal with negligible damping described by a real Drude metal. The black colored solid curves to the right side of the light lines (blue solid curve) correspond to the SPP excitation due to their bound nature. In this region for large wave vectors the frequency of the SPP approaches a characteristic surface plasmon frequency [17].

$$\omega_{sp} = \frac{\omega_p}{\sqrt{1+\varepsilon_2}} \tag{14}$$

The discussion so far assumed an ideal conductor where $Im[\varepsilon_1] = 0$ whereas real metals suffer from both free electron and inter-band damping. As a result, the propagating SPPs get damped with an energy attenuation length $L = (2Im[\beta])^{-1}$ which is usually between 10 and 100 μm for visible light. In the case of real metals, bound SPPs approaches a finite wave vector value at ω_{sp}. This results in a lower bound for the wavelength of the surface plasmon. In practical SPR sensors there are alternative conducting and dielectric thin films. Each interface sustains a bound SPP. For thin layers which are smaller or comparable to the decay length interactions between adjacent SPPs result in coupled modes. For an insulator-metal-insulator (IMI) heterostructure a general description of the TM mode can be described as follows.

For $z > a$

$$H_y = Ae^{i\beta x}e^{-k_3 z} \tag{15}$$

$$E_x = iA\frac{1}{\omega\varepsilon_0\varepsilon_3}k_3 e^{i\beta x}e^{-k_3 z} \tag{16}$$

$$E_z = -A\frac{\beta}{\omega\varepsilon_0\varepsilon_3}e^{i\beta x}e^{-k_3 z} \tag{17}$$

And for $z < -a$

$$H_y = Be^{i\beta x}e^{k_2 z} \tag{18}$$

$$E_x = -iB\frac{1}{\omega\varepsilon_0\varepsilon_2}k_2 e^{i\beta x}e^{k_2 z} \tag{19}$$

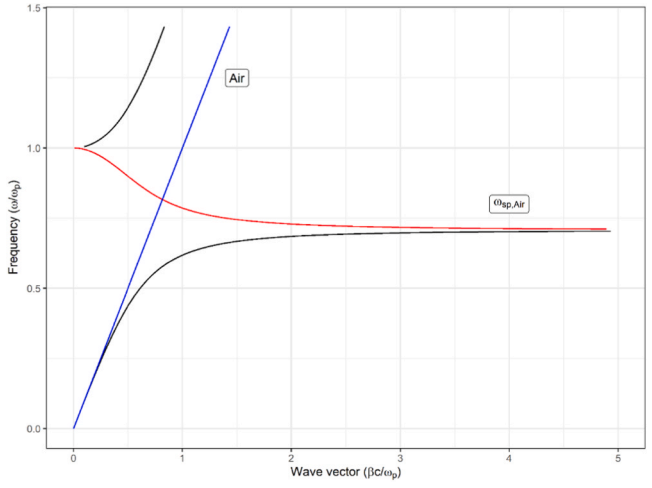

Fig. 2. Dispersion relationship (DR) of a SPP in a Drude metal – air interface, Re [DR] – black curve, Im [DR] – red curve, light curve – blue curve.

$$E_z = -B\frac{\beta}{\omega\varepsilon_0\varepsilon_2}e^{i\beta x}e^{k_2 z} \tag{20}$$

Inside the metal core modes from both interfaces couples and results in

$$H_y = Ce^{i\beta x}e^{-k_1 z} + De^{i\beta x}e^{k_1 z} \tag{21}$$

$$E_x = iC\frac{1}{\omega\varepsilon_0\varepsilon_1}k_1 e^{i\beta x}e^{-k_1 z} - iD\frac{1}{\omega\varepsilon_0\varepsilon_1}k_1 e^{i\beta x}e^{k_1 z} \tag{22}$$

$$E_z = C\frac{\beta}{\omega\varepsilon_0\varepsilon_1}e^{i\beta x}e^{-k_1 z} + D\frac{\beta}{\omega\varepsilon_0\varepsilon_1}e^{i\beta x}e^{k_1 z} \tag{23}$$

Applying the necessary boundary conditions and solving the resulting system of linear equations results in a dispersion relationship as follows.

$$e^{-4k_1 a} = \begin{matrix} \frac{k_1}{\varepsilon_1}+\frac{k_2}{\varepsilon_2} & \frac{k_1}{\varepsilon_1}+\frac{k_3}{\varepsilon_3} \\ \frac{k_1}{\varepsilon_1}-\frac{k_2}{\varepsilon_2} & \frac{k_1}{\varepsilon_1}-\frac{k_3}{\varepsilon_3} \end{matrix} \tag{24}$$

Excitation of SPPs using light is difficult because bound states of SPP's have higher wave vectors than the light line does i.e., $k_x > \omega/c$. At a given photon energy of $\hbar\omega$ the wave vector becomes $\hbar\omega/c$ and it should be increased by a Δk_x amount [18].

3. Configurations for SPR biosensing

As the refractive index of the superstrate changes in a SPR sensor, the propagation constant of the surface plasmon varies as well. This change triggers an alteration of the coupling between SP and incident light wave. As a result, different characteristics of the output optical wave change. These changes can be sensed and calibrated to the RI change in the superstrate. To track the changes, variations in wave angle, wavelength, phase, intensity and polarization is generally utilized.

SPR sensors with angular modulation use monochromatic light to excite the surface plasmons and the reflectance is measured as a function of the incident angle. The angle which has the strongest coupling shows a dip in the reflected light intensity and since it is sensitive to the superstrate's RI it can be calibrated to measure the RI change [19,20]. Theoretically a three layered Kretschmann setup with a prism, a metal layer and the sample layer is adequate for sensing purposes. But practical SPR sensors usually employ more than five layers. In most cases an additional sensing chip layer and a chromium layer are being used. Johansen et al. has theoretically and experimentally investigated the effects of a multilayer systems and how it could solve practical issues such as insufficient adhesion of gold on glass prism with first sputtering a thin chromium layer on a special glass substrate and using refractive index matching gel to connect the stack to the prism [21]. Zhou et al. has investigated how thickness of different metal layers can be optimized to obtain the most sensitivity out of an angular modulated SPR sensor [19].

Different light absorbing materials are being investigated in place of traditional sensing layer materials, these novel materials include silicon nanosheets, metal dichalcogenides and functionalized graphene layers and increased angular sensitivities also have been reported [22–24].

Zeng et al. have developed a rapid wavelength scanning SPR microscopy technique which is capable of real time sensing [25]. A liquid crystal tunable filter is utilized for fast scanning through wavelengths. Wavelength modulation is advantageous for fast scanning applications rather than angular modulation where mechanical scanning systems are used. Fiber optic SPR sensors now use graphene as the sensing layer due to its high surface-volume ratio and good biocompatibility [26]. Wei et al. has theoretically and experimentally investigated a graphene/gold enhanced fiber optic SPR sensor with wavelength modulation. This method employs a probe beam as well as a reference beam.

The phase shift $\Delta\varphi$ due to the interference with SPPs can be observed in their spatial displacement compared to one another [27]. The probe

beam shows the maximal phase variation at the dip of the SPR curve, whereas maximal amplitude change is on the resonance slopes. This makes the phase modulation method more sensitive to RI change than the amplitude change. One of the major obstacles of using phase modulators in SPR sensors is their sensitivity to temperature fluctuations and mechanical vibrations. Ye et al. [28] has developed a SPR biosensor array using a novel prism phase modulator to modulate the phase change between p and s polarized light. Due to increased stability the detection limit has improved to about 9.11×10^{-7} refractive index units (RIU).

The change of the polarization state of the totally reflected light at the interface is a result of two effects taking place 1. Change of TM reflectivity as a function of sample refractive index. 2. The phase shift added to the TM wave compared to the TE wave. Compared to the TM wave, TE wave only slightly changes in phase and amplitude. As a result, when a linearly polarized light is incident, the reflected light becomes elliptically polarized [29].

3.1. Prism method

Nylander and Liedberg published the first use of the SPR technique as a sensor in 1982 [11]. However, experimental studies utilizing SPR did not begin until Otto [30], Kretschmann and Raether [12] independently proved resonant optical excitations of surface plasmons using various attenuated total reflection setups. The most common SPR sensor configuration is the one that Kretschmann proposed using a prism.

Consider the interface of a metal and a dielectric. When light is reflected off the metal surface into the dielectric the photon momentum becomes $(\hbar\omega/c)\sqrt{\varepsilon_2}$ instead of $\hbar\omega/c$. Its projection of its wavevector parallel to the interface is $(\hbar\omega/c)\ \sqrt{\varepsilon_2}\ \sin(\theta)$. The excitation of surface plasmons happen in the vicinity of region of total internal reflection. An evanescent wave with a phase velocity of $\upsilon = \omega/\ k_x = c/\left(\sqrt{\varepsilon_2}\sin(\theta)\right)$ propagates as a result. since $\sqrt{\varepsilon_2}\sin(\theta)\rangle 1$ the propagating speed of SPP is less than the speed of light. Thus the resonant condition can be fulfilled. Under prism coupling two constructions are possible. 1. Metal layer can be seperated from the medium ε_0 using air or a dielectric layer illustrated by Fig. 3(b). 2. A metal layer with a thickness of seven hundred angstroms directly contact the ε_0 medium illustrated by Fig. 3 (a).

The minimum of the reflected intensity can be quantitatively figured out using the Fresnel's equations for a three dielectric layer system. In this system ε_0, ε_1 and ε_2 represents the dielectric constants of the prism, metal and air respectively. For an incident p polarized light, the reflectivity can be expressed as

$$R = \left|\frac{E_r^p}{E_r^p}\right|^2 = \left|\frac{r_{01}^p + r_{12}^p \exp(2ik_{z1}d)}{1 + r_{01}^p r_{12}^p \exp(2ik_{z1}d)}\right|^2 \tag{25}$$

$$r_{ik}^p = \left(\frac{k_{Zi}}{\varepsilon_i} - \frac{k_{zk}}{\varepsilon_k}\right) \Big/ \left(\frac{k_{zi}}{\varepsilon_i} + \frac{k_{zk}}{\varepsilon_k}\right) \tag{26}$$

Under conditions of $|\varepsilon_1^{'}| \gg 1$ and $|\varepsilon_1^{''}| \ll |\varepsilon_1^{'}|$ Eq. (25) can be simplified in the resonance region using a Lorentzian type of relationship

$$R = 1 - \frac{4\Gamma_i \Gamma_{rad}}{\left[k_x - \left(k_x^0 + \Delta k_x\right)\right]^2 + \left(\Gamma_i + \Gamma_{rad}\right)^2} \tag{27}$$

Prism coupling technique is also used to excite coupled surface plasmons in metal-dielectric-metal and dielectric-metal-dielectric layered systems. Quail et al. has used index matching oils to excite both high frequency ω_+ mode and low frequency ω_+ in dielectric-metal-dielectric structures using prism coupling [31].

Conventional SPR sensors with prism coupling that use metal layers like Ag, Au and Al does not often provide the sensitivity required for biosensors to detect very low levels of bio molecules. Thus, numerous studies are being carried out to enhance sensitivity. A common method of enhancing the sensitivity is to modify the sensing layer in terms of structure, geometry, and materials. Multiple layers with new materials such as graphene [32–35], Silicon [22,36,37] GSe and MXene ($Ti_3C_2T_x$) [22,38] have been utilized for this purpose.

Jia et al. has theoretically studied the effect of adding Gallium Sulfide layers to enhance the sensitivity of conventional SPR sensors consisting of gold, aluminum and silver metallic layers [39].

A theoretical simulation of the angular interrogation approach is used in the work of Kushwaha et al. to examine the performance of the hybrid SPR biosensor based on Zinc oxide (ZnO), gold, and graphene. In comparison to other traditional SPR biosensors that have been reported, they discovered that the proposed biosensor has a better sensitivity of 187.43°/RIU for the detection of pseudomonas-like bacteria. Additionally, they stated that ZnO is responsible for the greater change in resonance angle that results in a notable improvement in the sensitivity [40]. Kumar et al. investigated the sensitivity of a SPR biosensor by employing silicon and a hybrid nanostructure of MXene and black phosphorus ($Ti_3C_2T_x$). According to the findings, the proposed SPR structure reaches its highest sensitivity of 264°/RIU reporting a significant sensitivity improvement (by 127.58 %) over traditional SPR. The study claims that increased sensitivity is made possible by a combination of each layer's desirable characteristics, including silicon's high RI, black phosphorus's carrier confinement and high charge carrier mobility, MXene-large's biocompatibility and metallic conductivity [36].

Cai et al. has reported improved sensitivity by introducing a gold grating layer to the gold-based Prism Coupled SPR (PC-SPR) sensor. The performance of the sensor was studied both theoretically and experimentally. Fig. 4 illustrates simulation results of the proposed and conventional SPR sensors. It is revealed that the proposed structure improves the RI sensitivity by a considerable amount as a result of the co-coupling that occurs with localized surface plasmons in the Au

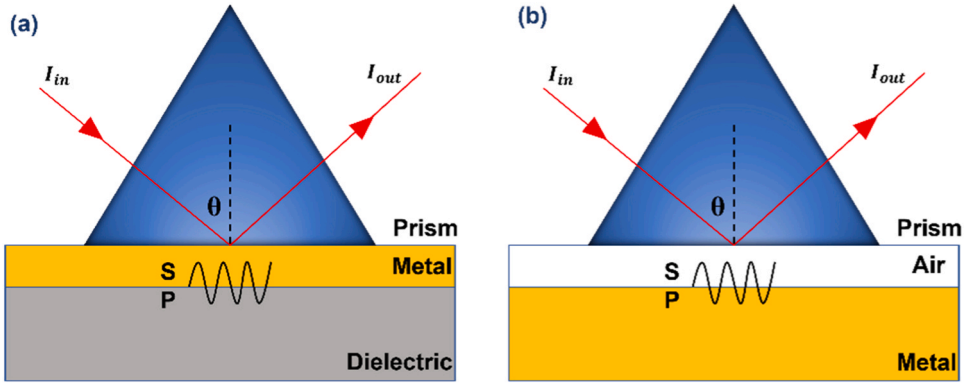

Fig. 3. Schematic diagram of excitation of surface plasmon polaritons using prism coupling in SPR biosensors (a) the Kretschmann configuration (b) the Otto configuration.

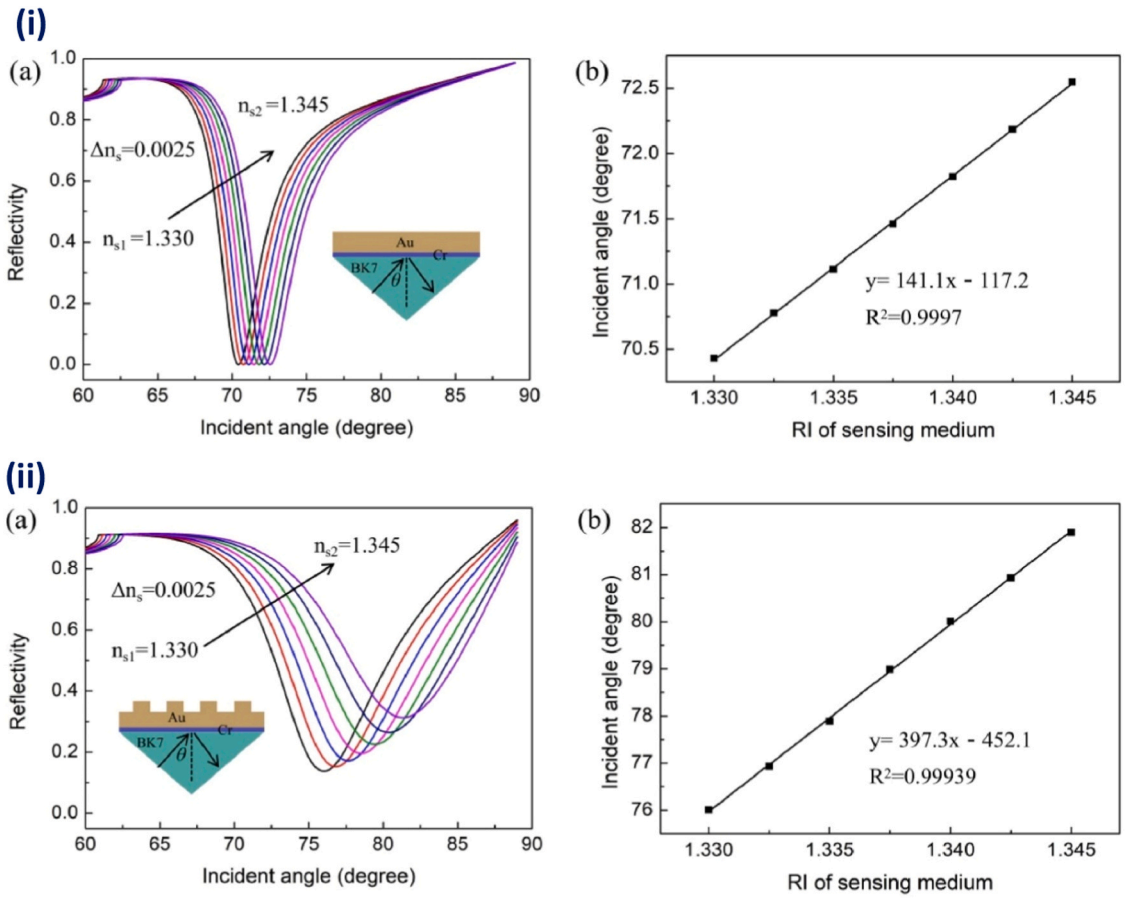

Fig. 4. (i) (a) SPR curve for conventional SPR sensor with the variation of RI of sensing medium; Insert: Schematic illustrations of the conventional SPR sensor (b) Linear regression analysis between the resonance angle and RI of sensing medium. (ii). (a) SPR curve for proposed SPR sensor with the variation of RI of sensing medium; Insert: Schematic illustrations of the proposed SPR sensor (b) Linear regression analysis between the resonance angle and RI of sensing medium. (Reprinted with permission from Ref. [41] © The Optical Society).

grating nanostructure apart from the SPPs propagating on the surface of gold layer [41]. In a study by Menon et al., they have improved the sensitivity for urea and creatinine in solutions selectively by introducing urease and creatininase enzymes to the analyte sample. This enhancement in sensitivity is believed to be due to the urea-urease and creatinine-creatininase coupling activity improving the RI of analyte sensing layer [42].

D. Michel et al. had suggested using a Concanavalin A coated nanolayer of gold in an SPR experimental setup to detect polysaccharides. The results showed that the SPR sensor was capable of accurately detecting polysaccharide molecules up to 0.22 g/L, including Xanthan gum. The double path architecture used by this optical SPR sensor makes optical alignment more sophisticated. Since the light interacts with the sensor material twice, the sensitivity can also be improved [43]. Kumbhat et al. has fabricated an SPR sensor for the detection of 17β-estradiol with the reported lowest detection of 10 pg/mL. They have used anti-estradiol acting as the interactant in a competitive inhibition immuno assay format which has led to the absence of interference from strong cross-reactants like progesterone and bisphenol-A indicating the high specificity and selectivity [44]. Karki et al. presented a modified conventional Kretschmann configuration, consisting of a BK7 prism, a dual silver layer, ZnO, MXene, and graphene as an SPR biosensor to measure the hemoglobin level in blood. According to the authors, it demonstrates that hemoglobin change may be identified with a sensitivity up to 161°/RIU and a 0.001 RI increment, corresponding to a 6.1025 g/L change in blood hemoglobin concentration [45].

3.2. Grating method

Fig. 5 is a general representation of the grating coupled SPR sensor configuration. When light hits a grating with a grating constant a at an angle of θ it's wave vector component parallel to the surface can be expressed as

$$k_x = \frac{\omega}{c}\sin\theta \pm \nu g = k_0\sqrt{\frac{\varepsilon_1\varepsilon_2}{\varepsilon_1+\varepsilon_2}} = k_{sp} \tag{28}$$

where ν is an integer and $g = 2\pi/a$. When the relationship in Eq. (28) is fulfilled, Incident light can excite a SPP.

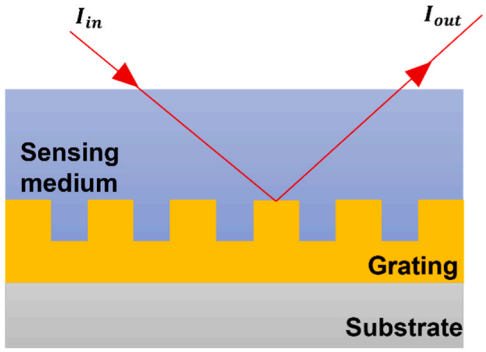

Fig. 5. Schematic diagram of excitation of surface plasmon polaritons using grating coupling in SPR biosensors.

Gratings have been used less than prisms in SPR sensors. But they offer a method of low-cost fabrication of SPR sensors. Gratings can be easily fabricated by replication into plastic substrates. Ruffato et al. has reported a grating coupled SPR sensor that uses polarization modulation [46]. Fig. 6 illustrates the experimental setup of the study. They have used the shift in phase of incident light to detect the binding of a specified analyte. The refractive index resolution of the system was found to be around 5×10^{-7}–1×10^{-6}. However, this value is directly related to the phase shift resolution of the detector. As a result, special attention must be given to improve the signal to noise ratio of the detector and data transmission of the sensor.

Prism structures were previously thought to be more sensitive and simpler to produce than grating structures [47]. Many publications have recently been published that demonstrate the remarkable sensitivity that grating-coupled plasmon resonance (GC-SPR) sensors can offer for TM polarized waves. Different strategies are utilized to increase the sensitivity in GC-SPR sensors such as employing gratings made of metals and dielectrics [48,49], multi-layer metal gratings [50–52] and gratings on semiconductor nanowires [53]. Additionally, by optimizing geometric grating characteristics like period, depth, and height the grating-based sensor's sensitivity can be increased [50,52,54,55].

Teotia and Kaler have proposed a GC-SPR waveguide biosensor for the Vroman effect-based detection of lung cancer biomarkers. A sharp resonance is produced by the suggested periodic grating made of multilayer metals, making it possible to identify cancerous cells early [52]. Dai et al. has experimentally showed that silver rectangular grating based SPR sensors can have higher sensitivity level compared to conventional PC-SPR sensor if the backward SPP is excited. Fig. 7 shows the experimental and theoretical reflectivity curves. In their study they have experimented with both positive order diffraction and negative order diffraction of gratings to excite forward SPPs and backward SPPs [49].

A sinusoidal Au-coated GaAs grating based SPR sensor has been the subject of theoretical and experimental study. According to Yaremchuk et al. two-layer grating that consists of gallium arsenide (GaAs) coated with a thin gold (Au) film is known to improve the sensitivity. Additionally, they used the rigorously coupled wave analysis simulation method to maximize Geometrical parameters [50].

In a study to detect Mycobacterium tuberculosis (MT) DNA, a limit of detection (LoD) down to 0.26 pM has been reported as a result of azimuthally controlled GC-SPR sensor and optimizing the peptide nucleic acid probe coating on the sensing layer [56]. Mendoza et al. has used dual-mode microarray method utilizing GC-SPR and grating-coupled surface plasmon coupled fluorescence (GCSPCF) imaging to detect circulating tumor cells [57].

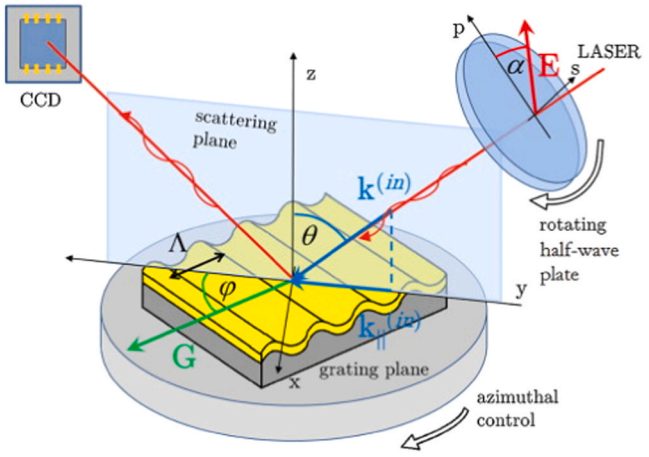

Fig. 6. Illustration of the experimental setup: fixed-wavelength laser ($\lambda = 635$ nm), rotating half-wave plate, plasmonic grating over a sample holder with azimuthal control, photodiode array (or CCD) for reflectivity collection connected to an electronic chain for data transduction. During the polarization-modulation analysis, polar and azimuthal angles (θ, ϕ) are kept fixed in correspondence of the plasmonic resonance and a polarization scan of the angle α is performed.
Reprinted with Permission from Ref. [46] (Elsevier).

A new SPR configuration has been developed by Jahanshahi and Adikan for improving the sensitivity of biosensors with highly absorbing molecules on the sensor surface. It comprises of a germanium nanowire grating coated with three layers of graphene. Additionally, the titanium layer that is added in between the gold and fused silica prevents the oxidation of the gold. This proposed structure has 60 % greater SPR angle resolution than the existing graphene based SPR structure according to the numerical analysis [53].

In a study for lipid molecule detection, the SPR sensors with basic Kretschmann configuration and a gold-based narrow groove grating were the subject of the study's optimization efforts. Using two different types of proteins as ligands, they studied the sensitivity variation in detecting two different types of lipids. It has been found that different combinations result in different limits of detection, with the phospholipid and tryptophan combination having the highest sensitivity at 900 nm/RIU in the infrared region increased [55].

3.3. Fiber optics

Use of optical fibers allows the fabrication of compact and miniature sensors that gives the exclusive advantage of taking localized measurements in hard to access locations. Fig. 8 is a schematic representation of a fiber optic SPR sensor. Two major sensor configurations exist for optical waveguide based SPR sensors namely, multimode optical fibers and single mode optical fibers. Jorgenson et al. has demonstrated the use of multimode optical fibers with an exposed core coated with a thin gold film [58]. Recently Jia et al. demonstrated how multi-mode optical fibers can be integrated with metallic nanohole arrays. They have developed their template transfer procedure from previous work in order to successfully integrate and ensure strong adhesion of nanostructures to the optical fiber tips [59]. The sensor configuration was then tested using water and NaCl solutions of various concentrations. The results revealed a prominent shift of peaks and troughs in the transmission spectra as the NaCl concentration changes. They have reported a sensitivity up to 559 nm/RIU [60].

Yet the multimode optical fiber inherits some major drawbacks such as modal and polarization conversion due to defects in the fiber. This in return reduces the stability and repeatability of the sensor. To overcome these challenges single mode optical fibers are being widely used that support only one EM mode thus preventing modal conversion. Coelho et al. has developed a single mode optical fiber SPR sensor with tapered cladding using chemical etching of the cladding and subsequent coating of Au and TiO_2. They have reported a sensitivity of 3800 nm/RIU for the reflection mode and a 5100 nm/RIU for the transmission mode. The transmission mode offered a higher sensitivity as it allows a single light path in the sensing region while the reflection mode allows a double path resulting in wider resonant dips [61].

SPR generation in gold-coated tilted fiber Bragg gratings (TFBGs) allows sensors to investigate the surrounding medium with near-infrared narrowband resonances, which improves both the evanescent field's penetration depth and the interrogation's wavelength resolution. TFBGs are gratings with RI modulation in short periods and are tilted with respect to the optical fiber axis. Christophe Caucheteur et al. has designed a near infrared grating assisted optical fiber SPR sensor that shows a spectral shift for RI changes higher than 1×10^{-2} RIU. They have analyzed the mode loss of the SPR sensor for different gold layer thicknesses from 10 to 100 nm. The simulations revealed that when the gold Au film is too thick, the SPP becomes uncoupled from the optical fiber and thus is impossible to excite. They have confirmed that the optimal performance is achieved for a thickness between 50 and 70 nm [62].

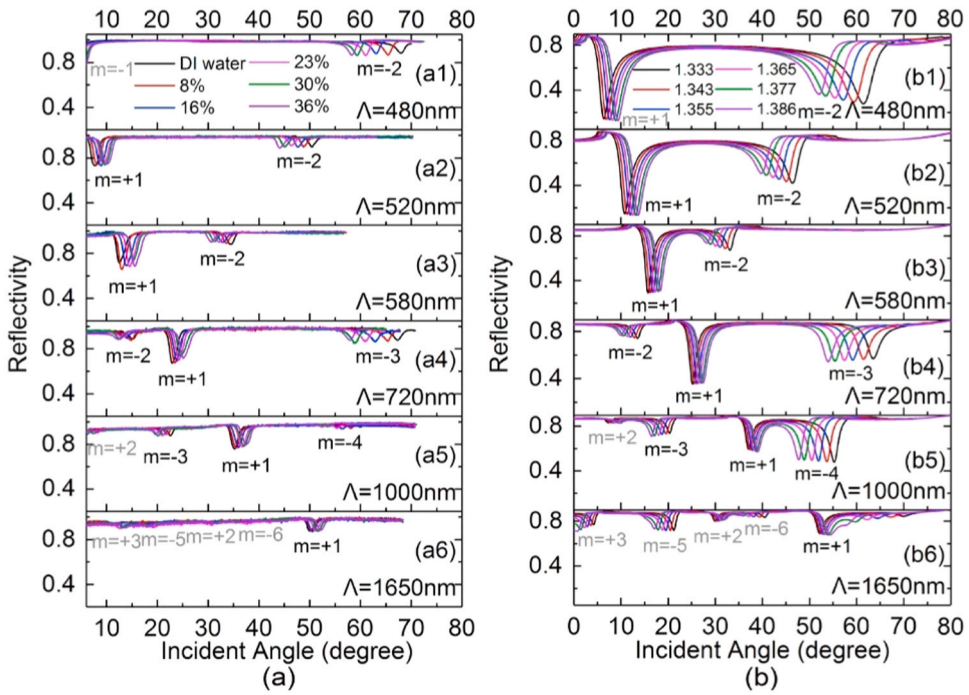

Fig. 7. a) Experimental reflectivity spectra of silver grating with different periods and the resonant dips in the reflectivity spectra move as the refractive index of the analyte change. (b) Theoretical reflectivity curves calculated by rigorous coupled-wave analysis method.
Reprinted with Permission from Ref. [49] (Elsevier).

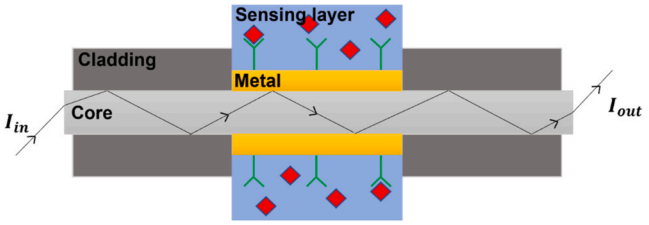

Fig. 8. Schematic diagram of fiber optic based SPR biosensors.

Recently, platinum has attracted a lot of attention as a noble metal that can excite SPPs. Jiang et al. has reported the first attempt to combine multilayer carbon nanotubes and platinum nanoparticle (MWCNT/PtNP) composites with the SPR technology. The optical fiber core with the gold coating is coated with MWCNT/PtNP using layer by layer self-assembled method. The refractive index sensitivity has been greatly increased up to 5923 nm/RIU compared to 1683 nm/RIU of a conventional SPR sensors with only an Au film [63].

Efforts have been made in recent years to increase the sensitivity of SPR sensors through two main approaches. One is to optimize the sensor structure and geometry and the other approach is to coat the metal film with different materials. Transition metal dichalcogenides (TMDC) such as MoS_2 and WS_2 have become a promising candidate for the SPR technology due to its high optical absorption efficiency, high specific surface area and good bio compatibility. Wang et al. and the group have fabricated and characterized a bimetallic optical fiber SPR based on Au/Ag followed by molybdenum disulfide (MoS_2) nanosheets coated on the metallic film. They have demonstrated experimentally and theoretically that MoS_2 can enhance the sensitivity of traditional bimetallic SPR sensors from 2487 nm/RIU to 3061 nm/RIU [64]. Wang et al. has shown both experimentally and theoretically integrating TiO_2 layer on top of gold layer improves the sensitivity to RI change and sensitivity increases with TiO_2 layer thickness [65].

Niu et al. has exploited the electric field intensity enhancement in the gap between gold nano particles and gold films. Finite element-based simulations revealed this gap field intensity is 4–5 times higher than that of near the Au film. Due to the coupling effect between SPR of the Au film and LSPR of the Au nanoparticles, the refractive index sensitivity of the D-type optical fiber SPR sensor has improved up to 3074 nm/RIU [66]. Li et al. and the group have developed an optical fiber based SPR biosensor to study DNA hybridization kinetics. The sensor is based on a D-shaped plastic optical fiber covered with an Au/Al_2O_3 composite hyperbolic metamaterial (HMM) structure and a graphene layer on the top layer. The graphene layer was functionalized with probe aptamer for DNA detection. The reported sensitivity is up to 4461 nm/RIU with a LoD down to 10 pM [67].

Food allergens such as peanut allergens can be deadly even in trace amounts inducing anaphylactic shock, therefore very sensitive biosensors are required to detect even the lowest quantities in complex food matrixes. The most widely used technique is enzyme-linked immunosorbent a planar assay (ELISA). Despite its versatility it is time consuming, not reusable, and difficult to automate. As an alternative Pollet et al. has reported the first attempt to incorporate nanobeads to signal enhancement in SPR sensors [68]. They have evaluated the system using a bioassay to detect Ara h1 peanut allergens in chocolate candy bars (Fig. 9). The results revealed how functionalized nanobeads can improve the detection limit of fiber optic SPR sensors. By utilizing magnetite nanoparticles labeling the detection limit has improved at least by two orders of magnitude from around 9–0.09 μg/mL. The detection limit of this SPR fiber sensor was found to be comparable to a commercial ELISA kit.

Cennamo et al. designed and fabricated a low-cost plastic optical fiber surface plasmon resonance (POF-SPR) biosensor to diagnose celiac disease. The formation of transglutaminase and anti-transglutaminase antibodies allow the diagnosis of celiac disease. In this study the gold film of the sensor was functionalized with guinea pig liver transglutaminase (tTG) to study the binding of anti-transglutaminase antibodies. They have reported the ability to sense a wide range of concentrations from 30 nM to 3000 nM [69]. Wang et al. has experimented using a fiber optic base SPR sensor modified using graphene oxide for human immunoglobulin G (IgG)detection. Furthermore, they

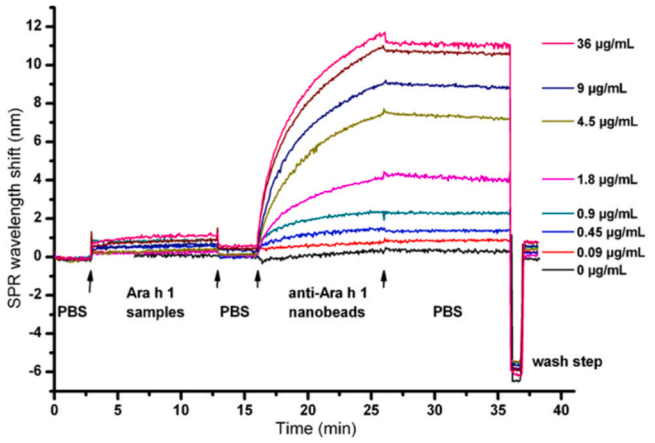

Fig. 9. SPR sensorgrams illustrating the binding of different concentrations of Ara h1, followed by an amplification step with nanoparticles functionalized with polyclonal antibodies. First the fiber was put for 3 min in the main buffer to stabilize and to acquire a baseline signal. Next, the fiber was dipped for 10 min in one of the samples, rinsed and placed again for 3 min in PBS buffer. Finally, the fiber was transferred to the vial with nanobeads to amplify the signal for 10 min. Desorption of the beads was monitored during 10 min of incubation in the PBS buffer. After each measurement the sensor was regenerated with a 2 min acid treatment.
Reprinted with Permission from Ref. [68] (Elsevier).

have used staphylococcal protein A that further enhance the sensitivity of the sensing layer by allowing directional immobilization of receptors promoting antigen–antibody binding efficiency [70].

3.4. Wave guide

The use of optical wave guides in SPR biosensors has become a popular trend due to the flexibility it provides when designing a miniaturized sensing element. Apart from being a rugged platform, it also supports multiple sensors to be built on a single chip. When coupled with optical fibers, wave guides provide means of remote sensing too. Fig. 10 shows a schematic of integrated optical waveguide (WG) SPR sensor.

The waveguide is locally covered by a planar stack sustaining the surface plasmons. To excite a surface plasmon by light propagating through a WG their phase velocities must match. The propagation constant of a SP depends heavily on the wavelength of incident light. Therefore, only a narrow band of the spectrum is capable of exciting SPPs. When polychromic light is introduced through the WG, the transmitted spectrum shows a narrow dip [71]. The sensitivity of conventional SPR sensors is limited in the visible region due to a broad spectrum caused by absorption losses in the metal layer.

Long Range Surface Plasmon-Polaritons (LRSPPs) are surface plasmon waves that travel relatively long distances along a metal layer in an Insulator-Metal-Insulator (IMI) configuration. The propagation length of LRSPP is around 2000 µm compared to 80 µm of a SPP in a single interface. The penetration depth of a LRSPP is about 1 µm which is around five times larger than that of a SPP. This characteristic is useful when probing relatively large biological targets such as cells. O. Krupin et al. has demonstrated the use of LSPP to detect the blood group antigen A on erythrocytes. The gold waveguides of the biosensor were functionalized with IgG immunoglobulin G by creating a self-assembled monolayer (SAM) of 16-mercaptohexadecanoic acid (16-MHA) and then conjugating the anti-A IgG through carbodiimide chemistry [72]. IMI structures that are capable of propagating LRSPPs are widely used to get a sharper resonance peak. Introduction of low index spacers between the metal layer and the WG has led to a new class of waveguides called hybrid plasmonic waveguides (HPWG). Nesterenko et al. has studied the sensitivity and resonance response of HPWG structures for S and P polarized light and has demonstrated that an optimal spacer thickness for sensing. In the absence of losses in WG and spacer a 10^5-fold increase in the sensitivity is reported compared to conventional SPR sensors [73].

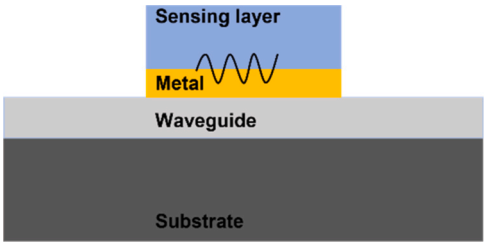

Fig. 10. Schematic diagram of excitation of surface plasmon polaritons using waveguide coupling in SPR biosensors.

SPR sensors that employ multimode planar wave guide structures have the advantage of being less sensitive to light coupling in and out of the structure due to the relatively large WG core. This aspect is very attractive for mass production of disposable lab on chip devices. However, in multimode waveguides different modes are coupled with SPP in different wavelengths. Thus, the resulting SPR spectrum is inherently broadened. Johanna et al. has addressed this issue by combining a multimode WG with an aptamer assisted gold nano particle sandwich assays. Fig. 11 shows the RI dependence of the transmission spectrum of the said SPR sensor. The chosen analyte is C-reactive protein (CRP). The reported sensitivity is 608.6 nm/RIU and it has a resolution of 4.3×10^{-3} RIU [74].

Wang et al. has developed a novel SPR biosensor with a carboxylate poly (N-isopropylacrylamide) hydrogel film attached to the metallic layer. The swollen hydrogel layer acts as the binding matrix as well as the wave guide. The reported hydrogel optical waveguide spectroscopy (HOWG) technique showed an order of magnitude improvement in the resolution of the SPR sensor as well as enhanced binding capacity. In this study, IgG molecules were detected with a limit of 10 pM LoD [75]. Molecules with small molecular weights are challenging to be detected using conventional WG modulated SPR sensors. Hedhly et al. has created a highly sensitive plasmonic biosensor for the detection of biomolecules using the symmetric metal cladding plasmonic waveguide (SMCW) structure. By carefully planning the arrangement and fine-tuning the thickness of the guiding layer, ultra-high order modes can be triggered. This results in a sharp phase change and a substantial position shift due to the Goos-Hänchen (GH) effect. This is the first example of biosensing based on GH shift measurement of a prism associated SMCW, attaining ultra-high sensitivity with a detection limit of 10^{-12} RIU. This SMCW structure enables a large electric field enhancement, leading in an increase in the GH shift from 18 µm to 284 µm [76].

Nano-porous metal oxide membranes have been attractive as a promising platform for sensitivity improvement in SPR sensors. Hotta et al. has demonstrated how sensitivity can be significantly improved using porous anodic alumina (PAA) waveguiding films. The careful optimization of thickness, porosity, and pore density of the PAA layer leads to enhanced adsorption of bovine serum albumin (BSA) analyte. This optimized sensor showed a large red shift in its SPR spectrum towards adsorption of BSA. The reported sensitivity is around 20-fold higher than that of the conventional SPR sensors [77].

Cennamo et al. has developed a low-cost WG SPR sensor using a tapered plastic optical fiber (POF) and molecularly imprinted polymer (MIP). This sensor has been used to detect small molecules such as L – nicotine (MW = 162.24). The sensor could differentiate between L and D nicotine. It is also shown that the sensitivity of this structure strongly depends on the geometry of tapered fiber. The reported sensitivity ranges from 1.3×10^4 nm/M, for a taper ratio 1.8–1.7×10^3 nm/M for a taper ratio of 1 [78]. Lee et al. has used a waveguide coupled bimetallic (WcBiM) SPR chip to detect amyloid-β42, which is considered as a biomarker for Alzheimer disease (AD). Early detection of AD is crucial for treating this disease. The SPR sensor offers a label free detection

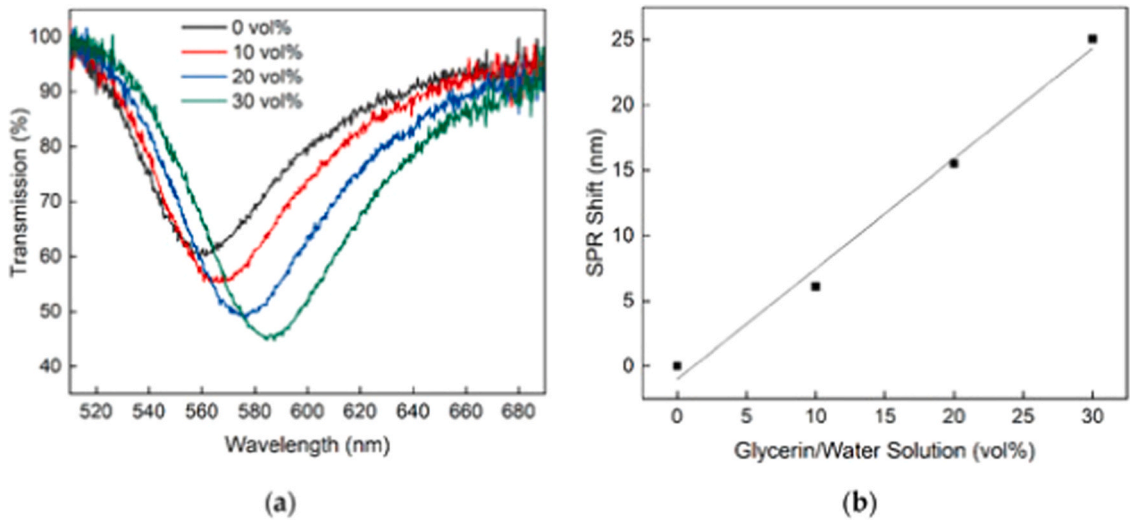

Fig. 11. Response of the planar-optical MM SPR waveguide sensor to different glycerin/water solutions. (**a**) The resulting transmission spectrum for different glycerin/water solutions and (**b**) the corresponding SPR wavelength shift for each transmission spectrum.
(From Ref. [74] MPDI. This article is an open access article distributed under the terms and conditions of the Creative Commons Attribution (CC BY) license).

technique free of interference occurring due to labeling process. The resolution of this WG-SPR sensor was enhanced by fixing the light source at a constant angle which gives the sharpest reflectance curve. For the selective detection of Aβ42, anti-Aβ42 was immobilized using a self-assembling monolayer [79].

Lee et al. has used their previously developed bimetallic waveguide-coupled surface plasmon resonance (Bi-WCSPR) sensor to detect CRP, a biomarker that is affiliated with inflammation in cardiovascular diseases. They have evaluated the performance of the Bi-WCSPR sensors with Ag – Au thickness ratios and have revealed that high Ag in the system improved the overall sensitivity. In the intensity interrogation mode, the LoD value of the Bi-WCSPR2 configuration was estimated to be 0.3034 g/mL, which was three times lower than the value obtained from the Au chip and an order of magnitude lower than the CRP cut-off level for cardiovascular events. These findings confirmed that Bi-WCSPR topologies offer a viable sensing platform for label-free identification of biomolecules at low concentrations [80].

4. Conclusion

In conclusion, SPR technology has improved over the past ten years, making it an important tool in medical diagnostics. It is now the approach of choice for many applications due to the sensitivity and specificity of SPR sensors in detecting biomolecular interactions. Table 1 summarizes a handful of such sensors with different configurations and analytes with the detection levels of those sensors. This review highlights the most recent advancements in SPR biosensor technology including strategies for increasing sensitivity and selectivity and its various configurations, including improvements in prism, grating, fiber optic, and waveguide modulated systems. Despite the progress made, there are still challenges that need to be addressed in order to further improve the performance and reliability of SPR biosensors in medical diagnostics. The continued advancement and optimization of SPR biosensors holds great promise for even greater applications in the future.

Declaration of Competing Interest

The authors declare that they have no known competing financial interests or personal relationships that could have appeared to influence the work reported in this paper.

Acknowledgements

We would like to express our gratitude to the Senate Research Committee (SRC) at the University of Moratuwa, Sri Lanka for their financial assistance under the Grant no. SRC/LT/2021/25.

Conflicts of interest

There are no conflicts to declare.

References

[1] C. de Martel, D. Georges, F. Bray, J. Ferlay, G.M. Clifford, Global burden of cancer attributable to infections in 2018: a worldwide incidence analysis, Lancet Glob. Health 8 (2020) e180–e190, https://doi.org/10.1016/S2214-109X(19)30488-7.
[2] M. Soler, C.S. Huertas, L.M. Lechuga, Label-free plasmonic biosensors for point-of-care diagnostics: a review, Expert Rev. Mol. Diagn. 19 (2019) 71–81, https://doi.org/10.1080/14737159.2019.1554435.
[3] L. Velmanickam, I.T. Lima, D. Nawarathna, Achieving over million-fold fluorescence enhancement for biosensing applications, in: Proceedings of the 2020 IEEE Research and Applications of Photonics in Defense Conference (RAPID), IEEE, 2020, pp. 1–2. ⟨https://doi.org/10.1109/RAPID49481.2020.9195707⟩.
[4] L. Velmanickam, M. Fondakowski, D. Nawarathna, Integrated dielectrophoresis and fluorescence-based platform for biomarker detection from serum samples, Biomed. Phys. Eng. Express 4 (2018), 025018, https://doi.org/10.1088/2057-1976/aaa516.
[5] L. Velmanickam, M. Bains, M. Fondakowski, G.P. Dorsam, D. Nawarathna, iLluminate-miRNA: paradigm for high-throughput, low-cost, and sensitive miRNA detection in serum samples at point-of-care, J. Phys. D Appl. Phys. 52 (2019), 055401, https://doi.org/10.1088/1361-6463/aaed97.
[6] A.B. Dahlin, B. Dielacher, P. Rajendran, K. Sugihara, T. Sannomiya, M. Zenobi-Wong, J. Vörös, Electrochemical plasmonic sensors, Anal. Bioanal. Chem. 402 (2012) 1773–1784, https://doi.org/10.1007/s00216-011-5404-6.
[7] L. Velmanickam, D. Nawarathna, Electric fields assisted fluorescence enhancement for microRNA biomarker detection in serum samples: strategies for combating cancer, obesity and addiction to opioid, in: B.M. Cullum, E.S. McLamore, D. Kiehl (Eds.), Smart Biomedical and Physiological Sensor Technology XVI, SPIE, 2019, p. 15, https://doi.org/10.1117/12.2520312.
[8] L. Velmanickam, M. Fondakowski, I.T. Lima, D. Nawarathna, Integrated dielectrophoretic and surface plasmonic platform for million-fold improvement in the detection of fluorescent events, Biomicrofluidics 11 (2017), 044115, https://doi.org/10.1063/1.5000008.
[9] E. Fort, S. Grésillon, Surface enhanced fluorescence, J. Phys. D Appl. Phys. 41 (2008), 013001, https://doi.org/10.1088/0022-3727/41/1/013001.
[10] P.L. Stiles, J.A. Dieringer, N.C. Shah, R.P. Van Duyne, Surface-enhanced Raman spectroscopy, Annu. Rev. Anal. Chem. 1 (2008) 601–626, https://doi.org/10.1146/annurev.anchem.1.031207.112814.
[11] B. Liedberg, C. Nylander, I. Lunström, Surface plasmon resonance for gas detection and biosensing, Sens. Actuators 4 (1983) 299–304, https://doi.org/10.1016/0250-6874(83)85036-7.

[12] E. Kretschmann, H. Raether, Notizen: radiative decay of non radiative surface plasmons excited by light, Z. Für Naturforsch. A 23 (1968) 2135–2136, https://doi.org/10.1515/zna-1968-1247.

[13] G. Steiner, Surface plasmon resonance imaging, Anal. Bioanal. Chem. 379 (2004) 328–331, https://doi.org/10.1007/s00216-004-2636-8.

[14] L. Velmanickam, I.T. Lima, D. Nawarathna, External low frequency electric fields maximize the fluorescence enhancement through light-metal-fluorophore interactions of target biomolecules, in: D.L. Farkas, J.F. Leary, A. Tarnok (Eds.), Imaging, Manipulation, and Analysis of Biomolecules, Cells, and Tissues XVII, SPIE, 2019, p. 28, https://doi.org/10.1117/12.2510137.

[15] J. Zhao, X. Zhang, C.R. Yonzon, A.J. Haes, R.P. Van Duyne, Localized surface plasmon resonance biosensors, Nanomedicine 1 (2006) 219–228, https://doi.org/10.2217/17435889.1.2.219.

[16] A. Abbas, M.J. Linman, Q. Cheng, Sensitivity comparison of surface plasmon resonance and plasmon-waveguide resonance biosensors, Sens. Actuators B Chem. 156 (2011) 169–175, https://doi.org/10.1016/j.snb.2011.04.008.

[17] M. Luo, Q. Wang, A reflective optical fiber SPR sensor with surface modified hemoglobin for dissolved oxygen detection, Alex. Eng. J. 60 (2021) 4115–4120, https://doi.org/10.1016/j.aej.2020.12.041.

[18] S.A. Maier, Plasmonics: Fundamentals and Applications, Springer US, New York, NY, 2007, https://doi.org/10.1007/0-387-37825-1.

[19] X. Zhou, K. Chen, L. Li, W. Peng, Q. Yu, Angle modulated surface plasmon resonance spectrometer for refractive index sensing with enhanced detection resolution, Opt. Commun. 382 (2017) 610–614, https://doi.org/10.1016/j.optcom.2016.08.030.

[20] H.R. Gwon, S.H. Lee, Spectral and angular responses of surface plasmon resonance based on the Kretschmann prism configuration, Mater. Trans. 51 (2010) 1150–1155, https://doi.org/10.2320/matertrans.M2010003.

[21] K. Johansen, H. Arwin, I. Lundström, B. Liedberg, Imaging surface plasmon resonance sensor based on multiple wavelengths: sensitivity considerations, Rev. Sci. Instrum. 71 (2000) 3530–3538, https://doi.org/10.1063/1.1287631.

[22] Q. Ouyang, S. Zeng, L. Jiang, L. Hong, G. Xu, X.Q. Dinh, J. Qian, S. He, J. Qu, P. Coquet, K.T. Yong, Sensitivity enhancement of transition metal dichalcogenides/silicon nanostructure-based surface plasmon resonance biosensor, Sci. Rep. 6 (1) (2016) 13, https://doi.org/10.1038/srep28190.

[23] Md.B. Hossain, Numerical modeling of MoS2–graphene bilayer-based high-performance surface plasmon resonance sensor: structure optimization for DNA hybridization, Opt. Eng. 59 (2020), https://doi.org/10.1117/1.OE.59.10.105105.

[24] N.-F. Chiu, S.-Y. Fan, C.-D. Yang, T.-Y. Huang, Carboxyl-functionalized graphene oxide composites as SPR biosensors with enhanced sensitivity for immunoaffinity detection, Biosens. Bioelectron. 89 (2017) 370–376, https://doi.org/10.1016/j.bios.2016.06.073.

[25] Y. Zeng, J. Zhou, X. Wang, Z. Cai, Y. Shao, Wavelength-scanning surface plasmon resonance microscopy: a novel tool for real time sensing of cell-substrate interactions, Biosens. Bioelectron. 145 (2019), 111717, https://doi.org/10.1016/j.bios.2019.111717.

[26] W. Wei, J. Nong, Y. Zhu, G. Zhang, N. Wang, S. Luo, N. Chen, G. Lan, C.-J. Chuang, Y. Huang, Graphene/Au-enhanced plastic clad silica fiber optic surface plasmon resonance sensor, Plasmonics 13 (2018) 483–491, https://doi.org/10.1007/s11468-017-0534-0.

[27] Y.H. Huang, H.P. Ho, S.K. Kong, A.V. Kabashin, Phase-sensitive surface plasmon resonance biosensors: methodology, instrumentation and applications, Ann. Phys. 524 (2012) 637–662, https://doi.org/10.1002/andp.201200203.

[28] G. Ye, W. Yang, L. Jiang, J. Qian, S. He, A novel phase-sensitive SPR biosensor array based on prism phase modulator, Smart Photon. Optoelectron. Integr. Circuits XVI 8989 (2014) 89890Q, https://doi.org/10.1117/12.2047367.

[29] M. Piliarik, J. Katainen, J. Homola, Novel polarization control for high-throughput surface plasmon resonance sensors, Opt. Sens. Technol. Appl. 6585 (2007), 658515, https://doi.org/10.1117/12.724462.

[30] A. Otto, Excitation of nonradiative surface plasma waves in silver by the method of frustrated total reflection, Z. Für Phys. A Hadrons Nucl. 216 (1968) 398–410, https://doi.org/10.1007/BF01391532.

[31] J.C. Quail, J.G. Rako, H.J. Simon, Long-range surface-plasmon modes in silver and aluminum films, Opt. Lett. 8 (1983) 377, https://doi.org/10.1364/OL.8.000377.

[32] M. Saifur Rahman, M.S. Anower, L.Bin Bashar, K.A. Rikta, Sensitivity analysis of graphene coated surface plasmon resonance biosensors for biosensing applications, Sens Biosens. Res. 16 (2017) 41–45, https://doi.org/10.1016/j.sbsr.2017.11.001.

[33] Md.B. Hossain, Numerical modeling of MoS2–graphene bilayer-based high-performance surface plasmon resonance sensor: structure optimization for DNA hybridization, Opt. Eng. 59 (2020), https://doi.org/10.1117/1.OE.59.10.105105.

[34] A. Verma, A. Prakash, R. Tripathi, Sensitivity enhancement of surface plasmon resonance biosensor using graphene and air gap, Opt. Commun. 357 (2015) 106–112, https://doi.org/10.1016/j.optcom.2015.08.076.

[35] M.B. Hossain, I.M. Mehedi, M. Moznuzzaman, L.F. Abdulrazak, M.A. Hossain, High performance refractive index SPR sensor modeling employing graphene tri sheets, Results Phys. 15 (2019), 102719, https://doi.org/10.1016/j.rinp.2019.102719.

[36] R. Kumar, S. Pal, A. Verma, Y.K. Prajapati, J.P. Saini, Effect of silicon on sensitivity of SPR biosensor using hybrid nanostructure of black phosphorus and MXene, Superlattices Microstruct. 145 (2020), 106591, https://doi.org/10.1016/j.spmi.2020.106591.

[37] R. Kumar, S. Pal, Y.K. Prajapati, J.P. Saini, Sensitivity enhancement of MXene based SPR sensor using silicon: theoretical analysis, Silicon 13 (2021) 1887–1894, https://doi.org/10.1007/s12633-020-00558-3.

[38] Y. Xu, Y. Ang, L. Wu, L. Ang, High sensitivity surface plasmon resonance sensor based on two-dimensional MXene and transition metal dichalcogenide: a theoretical study, Nanomaterials 9 (2019) 165, https://doi.org/10.3390/nano9020165.

[39] Y. Jia, Y. Liao, H. Cai, Sensitivity improvement of surface plasmon resonance biosensors with GeS-metal layers, Electronics 11 (2022), https://doi.org/10.3390/electronics11030332.

[40] A.S. Kushwaha, A. Kumar, R. Kumar, M. Srivastava, S.K. Srivastava, Zinc oxide, gold and graphene-based surface plasmon resonance (SPR) biosensor for detection of pseudomonas like bacteria: a comparative study, Optik 172 (2018) 697–707, https://doi.org/10.1016/j.ijleo.2018.07.066.

[41] H. Cai, M. Wang, J. Liu, X. Wang, Theoretical and experimental study of a highly sensitive SPR biosensor based on Au grating and Au film coupling structure, Opt. Express 30 (2022) 26136, https://doi.org/10.1364/OE.461768.

[42] P.S. Menon, F.A. Said, G.S. Mei, D.D. Berhanuddin, A.A. Umar, S. Shaari, B. Y. Majlis, Urea and creatinine detection on nano-laminated gold thin film using Kretschmann-based surface plasmon resonance biosensor, PLoS One 13 (2018), e0201228, https://doi.org/10.1371/journal.pone.0201228.

[43] D. Michel, F. Xiao, L. Skillman, K. Alameh, Surface plasmon resonance sensor for *in situ* detection of xanthan gum, IEEE J. Sel. Top. Quantum Electron. 22 (2016) 379–382, https://doi.org/10.1109/JSTQE.2015.2477054.

[44] S. Kumbhat, R. Gehlot, K. Sharma, U. Singh, V. Joshi, Surface plasmon resonance based indirect immunoassay for detection of 17β-estradiol, J. Pharm. Biomed. Anal. 163 (2019) 211–216, https://doi.org/10.1016/j.jpba.2018.10.015.

[45] B. Karki, B. Vasudevan, A. Uniyal, A. Pal, V. Srivastava, Hemoglobin detection in blood samples using a graphene-based surface plasmon resonance biosensor, Optik 270 (2022), 169947, https://doi.org/10.1016/j.ijleo.2022.169947.

[46] G. Ruffato, E. Pasqualotto, A. Sonato, G. Zacco, D. Silvestri, M. Morpurgo, A. De Toni, F. Romanato, Implementation and testing of a compact and high-resolution sensing device based on grating-coupled surface plasmon resonance with polarization modulation, Sens. Actuators B Chem. 185 (2013) 179–187, https://doi.org/10.1016/j.snb.2013.04.113.

[47] X.D. Hoa, A.G. Kirk, M. Tabrizian, Towards integrated and sensitive surface plasmon resonance biosensors: a review of recent progress, Biosens. Bioelectron. 23 (2007) 151–160, https://doi.org/10.1016/j.bios.2007.07.001.

[48] K.M. Byun, S.J. Kim, D. Kim, Grating-coupled transmission-type surface plasmon resonance sensors based on dielectric and metallic gratings, Appl. Opt. 46 (2007) 5703, https://doi.org/10.1364/AO.46.005703.

[49] Y. Dai, H. Xu, H. Wang, Y. Lu, P. Wang, Experimental demonstration of high sensitivity for silver rectangular grating-coupled surface plasmon resonance (SPR) sensing, Opt. Commun. 416 (2018) 66–70, https://doi.org/10.1016/j.optcom.2018.02.010.

[50] I. Yaremchuk, H. Petrovska, V. Fitio, Y. Bobitski, Optimization and fabrication of the gold-coated GaAs diffraction gratings for surface plasmon resonance sensors, Optik 158 (2018) 535–540, https://doi.org/10.1016/j.ijleo.2017.12.148.

[51] Wei Chen, Ling Guo, Zhijun Sun, Resonant absorption of TE-polarized light at the surface of a dielectric-coated metal grating, IEEE Photonics J. 6 (2014) 1–6, https://doi.org/10.1109/JPHOT.2014.2337893.

[52] P.K. Teotia, R.S. Kaler, 1-D grating based SPR biosensor for the detection of lung cancer biomarkers using Vroman effect, Opt. Commun. 406 (2018) 188–191, https://doi.org/10.1016/j.optcom.2017.03.079.

[53] P. Jahanshahi, F.R.M. Adikan, Sensitivity enhancement of graphene-based surface plasmon resonance biosensor using germanium nanowires grating, J. Med. Bioeng. 4 (2015) 145–149, https://doi.org/10.12720/jomb.4.2.145-149.

[54] S. Long, J. Cao, S. Geng, N. Xu, W. Qian, S. Gao, Optimization of plasmonic sensors based on sinusoidal and rectangular gratings, Opt. Commun. 476 (2020), 126310, https://doi.org/10.1016/j.optcom.2020.126310.

[55] E. Kabir, S.M.A. Uddin, S.S. Chowdhury, Optimization of surface plasmon resonance biosensor for analysis of lipid molecules, in: Proceedings of the 2020 2nd International Conference on Advanced Information and Communication Technology (ICAICT), IEEE, 2020, pp. 59–64. ⟨https://doi.org/10.1109/ICAICT51780.2020.9333462⟩.

[56] D. Silvestri, A. Sonato, G. Ruffato, A. Meneghello, A. Antognoli, E. Cretaio, M. Dettin, A. Zamuner, E. Casarin, G. Zacco, F. Romanato, M. Morpurgo, A peptide nucleic acid label-free biosensor for Mycobacterium tuberculosis DNA detection via azimuthally controlled grating-coupled SPR, Anal. Methods 7 (2015) 4173–4180, https://doi.org/10.1039/C5AY00277J.

[57] A. Mendoza, D.M. Torrisi, S. Sell, N.C. Cady, D.A. Lawrence, Grating coupled SPR microarray analysis of proteins and cells in blood from mice with breast cancer, Analyst 141 (2016) 704–712, https://doi.org/10.1039/C5AN01749A.

[58] R.C. Jorgenson, S.S. Yee, A fiber-optic chemical sensor based on surface plasmon resonance, Sens. Actuators B Chem. 12 (1993) 213–220, https://doi.org/10.1016/0925-4005(93)80021-3.

[59] P. Jia, H. Jiang, J. Sabarinathan, J. Yang, Plasmonic nanohole array sensors fabricated by template transfer with improved optical performance, Nanotechnology 24 (2013), 195501, https://doi.org/10.1088/0957-4484/24/19/195501.

[60] P. Jia, J. Yang, Integration of large-area metallic nanohole arrays with multimode optical fibers for surface plasmon resonance sensing, Appl. Phys. Lett. 102 (2013), 243107, https://doi.org/10.1063/1.4811700.

[61] L. Coelho, J.M.M.M. de Almeida, J.L. Santos, R.A.S. Ferreira, P.S. André, D. Viegas, Sensing structure based on surface plasmon resonance in chemically etched single mode optical fibres, Plasmonics 10 (2015) 319–327, https://doi.org/10.1007/s11468-014-9811-3.

[62] C. Caucheteur, V. Voisin, J. Albert, Near-infrared grating-assisted SPR optical fiber sensors: design rules for ultimate refractometric sensitivity, Opt. Express 23 (2015) 2918, https://doi.org/10.1364/OE.23.002918.

[63] X. Jiang, Q. Wang, Refractive index sensitivity enhancement of optical fiber SPR sensor utilizing layer of MWCNT/PtNPs composite, Opt. Fiber Technol. 51 (2019) 118–124, https://doi.org/10.1016/j.yofte.2019.05.007.
[64] Q. Wang, X. Jiang, L.-Y. Niu, X.-C. Fan, Enhanced sensitivity of bimetallic optical fiber SPR sensor based on MoS2 nanosheets, Opt. Lasers Eng. 128 (2020), 105997, https://doi.org/10.1016/j.optlaseng.2019.105997.
[65] T. Wang, M. Zhang, K. Liu, J. Jiang, Y. Zhao, J. Ma, T. Liu, The effect of the TiO2 film on the performance of the optical fiber SPR sensor, Opt. Commun. 448 (2019) 93–97, https://doi.org/10.1016/j.optcom.2019.05.023.
[66] L.Y. Niu, Q. Wang, J.Y. Jing, W.M. Zhao, Sensitivity enhanced D-type large-core fiber SPR sensor based on gold nanoparticle/Au film co-modification, Opt. Commun. 450 (2019) 287–295, https://doi.org/10.1016/j.optcom.2019.06.026.
[67] C. Li, J. Gao, M. Shafi, R. Liu, Z. Zha, D. Feng, M. Liu, X. Du, W. Yue, S. Jiang, Optical fiber SPR biosensor complying with a 3D composite hyperbolic metamaterial and a graphene film, Photonics Res. 9 (2021) 379, https://doi.org/10.1364/PRJ.416815.
[68] J. Pollet, F. Delport, K.P.F. Janssen, D.T. Tran, J. Wouters, T. Verbiest, J. Lammertyn, Fast and accurate peanut allergen detection with nanobead enhanced optical fiber SPR biosensor, Talanta 83 (2011) 1436–1441, https://doi.org/10.1016/j.talanta.2010.11.032.
[69] N. Cennamo, A. Varriale, A. Pennacchio, M. Staiano, D. Massarotti, L. Zeni, S. DAuria, S. D'Auria, An innovative plastic optical fiber-based biosensor for new bio/applications. the case of celiac disease, Sens. Actuators B Chem. 176 (2013) 1008–1014, https://doi.org/10.1016/j.snb.2012.10.055.
[70] Q. Wang, J.-Y. Jing, B.-T. Wang, Highly sensitive SPR biosensor based on graphene oxide and staphylococcal protein A co-modified TFBG for human IgG detection, IEEE Trans. Instrum. Meas. 68 (2019) 3350–3357, https://doi.org/10.1109/TIM.2018.2875961.
[71] J. Dostálek, J. Čtyroký, J. Homola, E. Brynda, M. Skalský, P. Nekvindová, J. Špirková, J. Škvor, J. Schröfel, Surface plasmon resonance biosensor based on integrated optical waveguide, Sens. Actuators B Chem. 76 (2001) 8–12, https://doi.org/10.1016/S0925-4005(01)00559-7.
[72] O. Krupin, C. Wang, P. Berini, Selective capture of human red blood cells based on blood group using long-range surface plasmon waveguides, Biosens. Bioelectron. 53 (2014) 117–122, https://doi.org/10.1016/j.bios.2013.09.051.
[73] D.V. Nesterenko, S. Hayashi, Z. Sekkat, Extremely narrow resonances, giant sensitivity and field enhancement in low-loss waveguide sensors, J. Opt. 18 (2016) 1–12, https://doi.org/10.1088/2040-8978/18/6/065004.
[74] J.-G. Walter, A. Eilers, L. Alwis, B. Roth, K. Bremer, SPR biosensor based on polymer multi-mode optical waveguide and nanoparticle signal enhancement, Sensors 20 (2020) 2889, https://doi.org/10.3390/s20102889.
[75] Y. Wang, C.-J. Huang, U. Jonas, T. Wei, J. Dostalek, W. Knoll, Biosensor based on hydrogel optical waveguide spectroscopy, Biosens. Bioelectron. 25 (2010) 1663–1668, https://doi.org/10.1016/j.bios.2009.12.003.
[76] M. Hedhly, Y. Wang, S. Zeng, F. Ouerghi, J. Zhou, G. Humbert, Highly sensitive plasmonic waveguide biosensor based on phase singularity-enhanced Goos–Hänchen shift, Biosensors 12 (2022) 457, https://doi.org/10.3390/bios12070457.
[77] K. Hotta, A. Yamaguchi, N. Teramae, Nanoporous waveguide sensor with optimized nanoarchitectures for highly sensitive label-free biosensing, ACS Nano 6 (2012) 1541–1547, https://doi.org/10.1021/nn204494z.
[78] N. Cennamo, G. D'Agostino, M. Pesavento, L. Zeni, High selectivity and sensitivity sensor based on MIP and SPR in tapered plastic optical fibers for the detection of l-nicotine, Sens. Actuators B Chem. 191 (2014) 529–536, https://doi.org/10.1016/j.snb.2013.10.067.
[79] Y.K. Lee, K. Lee, W.M. Kim, Y. Sohn, Detection of amyloid-β42 using a waveguide-coupled bimetallic surface plasmon resonance sensor chip in the intensity measurement mode, PLoS One 9 (2014) 1–7, https://doi.org/10.1371/journal.pone.0098992.
[80] H.-S. Lee, T.-Y. Seong, W.M. Kim, I. Kim, G.-W. Hwang, W.S. Lee, K.-S. Lee, Enhanced resolution of a surface plasmon resonance sensor detecting C-reactive protein via a bimetallic waveguide-coupled mode approach, Sens. Actuators B Chem. 266 (2018) 311–317, https://doi.org/10.1016/j.snb.2018.03.136.
[81] M. Soler, M.-C. Estevez, M. de L. Moreno, A. Cebolla, L.M. Lechuga, Label-free SPR detection of gluten peptides in urine for non-invasive celiac disease follow-up, Biosens. Bioelectron. 79 (2016) 158–164, https://doi.org/10.1016/j.bios.2015.11.097.
[82] W. Gong, S. Jiang, Z. Li, C. Li, J. Xu, J. Pan, Y. Huo, B. Man, A. Liu, C. Zhang, Experimental and theoretical investigation for surface plasmon resonance biosensor based on graphene/Au film/D-POF, Opt. Express 27 (2019) 3483, https://doi.org/10.1364/OE.27.003483.
[83] B. Sciacca, A. François, P. Hoffmann, T.M. Monro, Multiplexing of radiative-surface plasmon resonance for the detection of gastric cancer biomarkers in a single optical fiber, Sens. Actuators B Chem. 183 (2013) 454–458, https://doi.org/10.1016/j.snb.2013.03.131.
[84] M.K. Alam, V. Dhasarathan, A. Natesan, R. Nambi, M.U. Zaman, K.K. Ganji, R. Basri, M.S. Munisekhar, A.K. Nagarajappa, H. Abutayyem, Human teeth disease detection using refractive index based surface plasmon resonance biosensor, Coatings 12 (2022) 1398, https://doi.org/10.3390/coatings12101398.
[85] Z.-W. Yang, T.-T.-H. Pham, C.-C. Hsu, C.-H. Lien, Q.-H. Phan, Single-layer-graphene-coated and gold-film-based surface plasmon resonance prism coupler sensor for immunoglobulin G detection, Sensors 22 (2022) 1362, https://doi.org/10.3390/s22041362.